Chemical Science

Accepted Manuscript

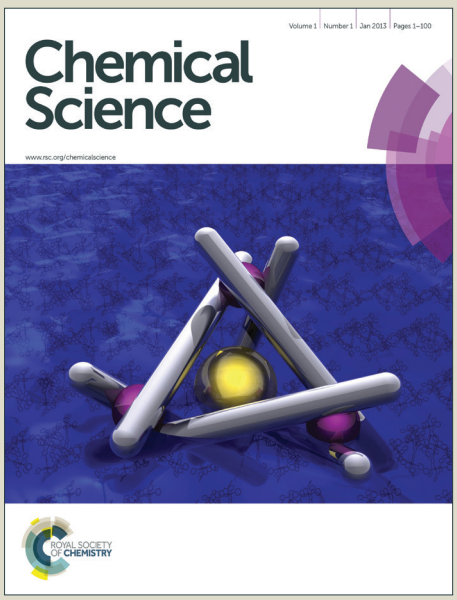

ROYAL SOCIETY OF CHEMISTRY

www.rsc.org/chemicalscience

Journal Name

RSCPublishing

ARTICLE

Secondary Stereocontrolling Interactions in Chiral Brønsted Acid Catalysis: Study of a Petasis-Ferrier-Type Rearrangement Catalyzed by Chiral Phosphoric Acids

Cite this: DOI: 10.1039/xoxxoooooox

Received ooth January 2012,
Accepted ooth January 2012

DOI: 10.1039/xoxxoooooox

www.rsc.org/

Kyohei Kanomata,[a] Yasunori Toda,[a] Yukihiro Shibata,[b] Masahiro Yamanaka,[b] Seiji Tsuzuki,[c] Ilya D. Gridnev[a] and Masahiro Terada*[a,d]

Chiral phosphoric acids have emerged as promising asymmetric Brønsted acid catalysts that harness hydrogen bonding interactions as key stereocontrolling elements. A new approach to chiral phosphoric acid catalysis through ion-paring interactions between the anionic conjugate base of the catalyst and a cationic electrophile has recently received attention. However, the mechanism of stereocontrol through ion-pairing interactions is still elusive. As a probe reaction for studying the stereocontrolling element involved in such catalytic reactions, we investigated the Petasis-Ferrier-type rearrangement of a 7-membered cyclic vinyl acetal catalyzed by chiral phosphoric acids. DFT calculations suggested that non-classical C-H···O hydrogen bonds between the catalyst and the substrate play an important role in determining the stereoselectivity. In addition, π-π stacking interactions were found to be a key factor for stereocontrol when using a 9-anthryl group-bearing catalyst.

Introduction

Chiral Brønsted acid catalysis has emerged as a rapidly growing area of research in recent years.[1] A variety of acid functionalities have been utilized in this context in combination with appropriate chiral sources. Among them, BINOL-derived axially chiral phosphoric acid catalysts **1** represent a highly efficient and widely applicable class of catalysts that enable a variety of organic transformations in a highly enantioselective fashion.[2] In chiral phosphoric acid-catalyzed reactions, hydrogen-bonding (or ion-pairing) interactions play a key role in controlling the stereochemical outcomes, and these reactions take place in the chiral environment created by the catalyst. Several computational studies of the reaction mechanisms and transition structures for chiral phosphoric acid catalyzed reactions have suggested that two-point hydrogen-bonding interactions are crucial for achieving high stereoselectivities; the acidic proton (P-OH) and the phosphoryl oxygen (P=O) of the catalyst simultaneously form X-H···A-type (X, A = heteroatom) hydrogen bonds that direct the orientations of the electrophile and nucleophile, respectively (Fig. 1a, **I**).[3-9]

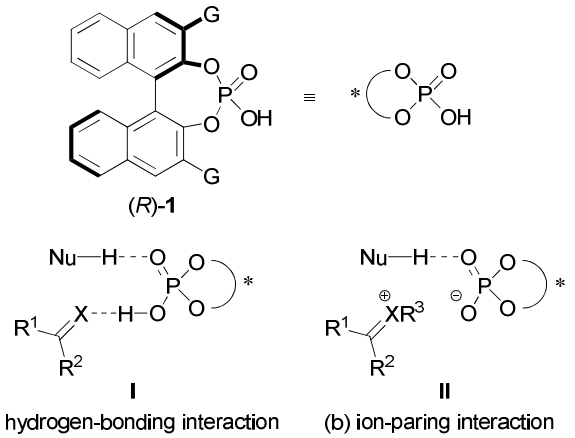

Fig. 1 Asymmetric activation mode of chiral phosphoric acid catalysis. (a) A neutral electrophile forms a hydrogen bond with a catalyst. (b) A cationic electrophile lacking a Brønsted basic site forms an ion-pair with anionic conjugate base of a catalyst. X = NR, O, etc. R^3, R ≠ H.

In recently reported protocols of chiral phosphoric acid catalysis, a high degree of enantioselectivity was attained through an ion-pair of positively charged electrophile and a negatively charged

conjugate base of the catalyst (Fig. 1b, **II**).[10-11] In these transformations, the electrophilic species lack acceptor sites for X-H···A-type hydrogen bond formation, which is considered essential for directing the electrophilic species. As a result, the stereocontrolling element in the ion-pair **II** is elusive.[12] A detailed understanding of the stereocontrolling elements in these catalytic reactions should not only shed light on the origin of stereoselectivity, but also enable the rational design of new catalysts and transformations.[13]

Oxocarbenium ions, which are thought to be involved in a wide range of fundamental transformations, are representative of cationic electrophilic species that lack X-H···A-type hydrogen bonding sites. In this context, we focused on the Petasis-Ferrier-type rearrangement[14,15] as an ideal probe for elucidating the stereocontrolling elements in the interaction between a positively charged electrophile and the negatively charged conjugate base of a chiral phosphoric acid catalyst (Scheme 1), because this rearrangement is proposed to proceed *via* a cationic oxocarbenium intermediate in the presence of an acid catalyst. The 7-membered cyclic vinyl acetal **2** was chosen as the substrate[16] based on the following considerations: (i) the stereochemical relationship between the starting material **2** and the product **3** has been well established, i.e., the reaction generally proceeds with retention of chirality[17] and (ii) substrate **2** has limited conformational flexibility because the nucleophilic and the electrophilic moieties are tethered with each other. Both of these features were expected to simplify the transition-structure analysis with respect to the oxocarbenium intermediate. Herein, we report the results of experimental and computational studies of the chiral phosphoric acid-catalyzed Petasis-Ferrier-type rearrangement of **2**. Guided by computational studies, the existence of non-classical C-H···O hydrogen bonds between the catalyst and the substrate is disclosed. The contribution of π-π stacking interactions in stabilizing a transition state is also proposed when using a 9-anthryl group-bearing catalyst.

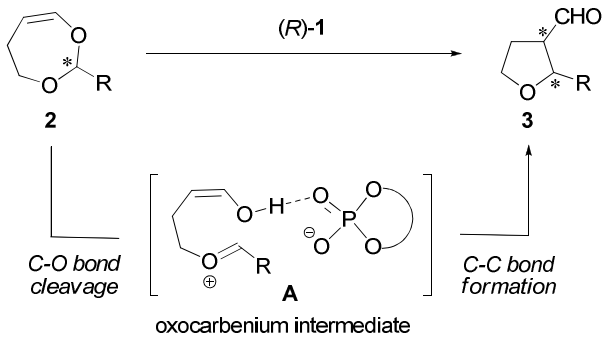

Scheme 1 Petasis-Ferrier-type rearrangement of cyclic vinyl acetals catalyzed by a chiral phosphoric acid.

Results and Discussion

■ Development of a Stereoselective Petasis-Ferrier-Type Rearrangement Catalyzed by Chiral Phosphoric Acids

To establish the reaction conditions for the mechanistic study, we began by exploring the Petasis-Ferrier-type rearrangement of enantiomerically pure 7-membered cyclic vinyl acetal (*R*)-**2a** (R = Ph). The initial reaction was performed with (*R*)-**2a** and 5 mol% chiral phosphoric acid catalyst (*R*)-**1a** (G = $SiPh_3$) in dichloromethane at 25 °C. The resulting aldehyde **3a** was reduced to the corresponding alcohol **4a** by treatment with sodium borohydride in one-pot in order to determine the yield, the diastereoselectivity, and the enantiomeric purity. The reaction proceeded smoothly, affording the desired product **4a** in moderate yield with high *anti*-selectivity (Table 1, entry 1). As expected, the chirality of the acetal carbon of the starting material (*R*)-**2a** was retained in the major diastereomer (*anti*-**4a**), albeit with a slight loss of enantiomeric purity.[18] Further screening of the substituent (G) of catalyst (*R*)-**1** revealed that the substituents significantly influenced the yield, the diastereoselectivity, and the degree of chirality transfer in the reaction (Table 1, entries 2 and 3). Catalyst (*R*)-**1b** (G = 2,4,6-(i-Pr)$_3$C$_6$H$_2$) and (*R*)-**1c** (G = 9-anthryl) decreased both the diastereoselectivity and the degree of chirality transfer compared to those of catalyst (*R*)-**1a** (Table1, entries 2 and 3 vs. entry 1), although both the major *anti*- and minor *syn*-diastereomers exhibited retention of chirality. Changing the solvent from dichloromethane to toluene further improved both the yield and diastereoselectivity using (*R*)-**1a**, although a longer reaction time was required to complete the reaction (Table 1, entry 1 vs. entry 4).[19] It should be noted that introduction of the substituent (G) at the 3,3'-position of the catalyst's binaphthyl backbone led to the formation of *anti*-**4a** as the major product in all cases examined (Table 1, entries 1-4). In contrast, the use of catalyst (*R*)-**1d** (G = H) with no substituent at the 3,3'-position resulted in almost no diastereoselectivity, along with a considerable decrease in the enantiomeric purity during the course of the reaction (Table 1, entry 5).[20] These results clearly suggest that the substituent (G) of the catalyst (*R*)-**1** plays a significant role in not only determining the diastereoselectivity, but also enabling retention of enantiomeric purity throughout the reaction.

Table 1 Petasis-Ferrier-type rearrangement of (*R*)-**2a** catalyzed by (*R*)-**1**[a]

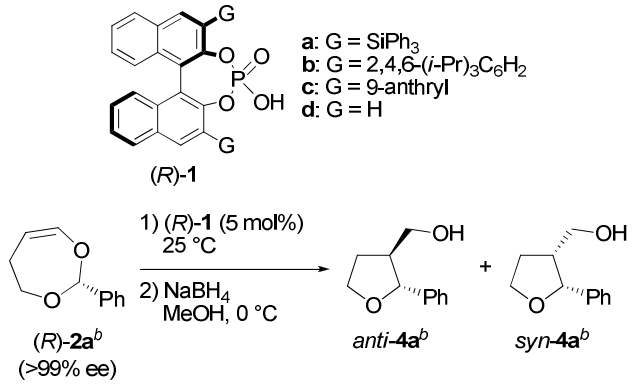

Entry	(*R*)-**1**	Solvent	*t* (h)	Yield (%)[c]	*anti*-**4a**/ *syn*-**4a**[d]	ee (%) for *anti*-**4a**[d]
1	**1a**	CH_2Cl_2	5	77	96:4	92
2	**1b**	CH_2Cl_2	1	76	88:12	79
3	**1c**	CH_2Cl_2	1	92	74:26	89
4	**1a**	toluene	12	95	99:1	95
5	**1d**	CH_2Cl_2	1	99	52:48	86

[a] All reactions were carried out with 0.005 mmol (*R*)-**1** (5 mol%) and 0.1 mmol (*R*)-**2a** (>99% ee) in solvent (0.5 mL) at 25 °C for the indicated time. [b] See ESI† for determination of the absolute configurations. [c] Combined yield of *anti*/*syn*-**4a**. [d] The diastereomeric ratio and enantiomeric excess were determined by chiral stationary phase HPLC analysis.

Next, the reaction of (*S*)-**2a** was conducted using conditions identical to those used for Table 1, entry 1. The reaction proceeded in good yield to provide the desired product **4a** after reduction with sodium borohydride (Table 2, entry 1).[19] As with (*R*)-**2a**, the reaction of (*S*)-**2a** in the presence of catalyst (*R*)-**1a** proceeded with *anti*-selectivity and retention of the chirality, albeit with considerable loss of enantiomeric purity for the major *anti*-**4a** product (from >99% ee to 72% ee) and only a slight loss of enantiomeric purity for the minor *syn*-**4a** (from >99% ee to 95% ee). Employment of catalyst (*R*)-**1b** led to a considerable reduction in the diastereoselectivity despite a high degree of chirality transfer (Table 2, entry 2). Interestingly, the reaction catalyzed by (*R*)-**1c** afforded *syn*-**4a** as the major product in moderate yield (Table 2, entry 3) with near-perfect retention of chirality on the acetal carbon of the starting material (*S*)-**2a**.[18] Changing the solvent from dichloromethane to toluene further improved both the *syn*-selectivity and the yield (Table 2, entry 3 vs. entry 4).[21] The particular *syn*-selectivity with catalyst (*R*)-**1c** strongly suggests that some unique stereocontrolling elements are involved in the present catalytic reaction. Furthermore, as observed for the reaction of (*R*)-**2a** catalyzed by (*R*)-**1d** (G = H) (Table 1, entry 5), the reaction of (*S*)-**2a** using (*R*)-**1d** also displayed almost no diastereoselectivity and considerable loss of enantiomeric purity during the course of the reaction (Table 2, entry 5).

Table 2 Petasis-Ferrier-type rearrangement of (*S*)-**2a** catalyzed by (*R*)-**1**[a]

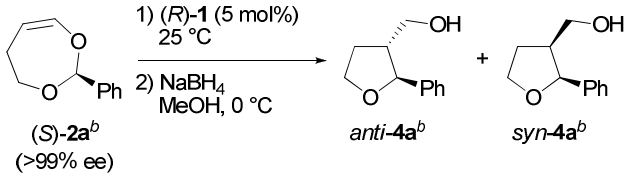

Entry	(*R*)-**1**	Solvent	*t* (h)	Yield (%)[c]	*anti*-**4a**/ *syn*-**4a**[d]	ee (%) for *syn*-**4a**[d]
1	**1a**	CH_2Cl_2	5	86	89:11[e]	95
2	**1b**	CH_2Cl_2	1	75	47:53	97
3	**1c**	CH_2Cl_2	1	75	16:84	98
4	**1c**	toluene	0.2	90	7:93	98
5	**1d**	CH_2Cl_2	1	98	49:51	76

[a] All reactions were carried out with 0.005 mmol (*R*)-**1** (5 mol%) and 0.1 mmol (*S*)-**2a** (>99% ee) in solvent (0.5 mL) at 25 °C for the indicated time. [b] See ESI† for determination of the absolute configurations. [c] Combined yield of *anti*/*syn*-**4a**. [d] The diastereomeric ratio and enantiomeric excess were determined by chiral stationary phase HPLC analysis. [e] 72% ee for *anti*-**4a**.

Briefly summarizing the experimental results, the reaction of (*R*)-**2a** in the presence of catalyst (*R*)-**1a** afforded *anti*-**4a** as the major product (Table 1, entry 4), while the reaction of (*S*)-**2a** in the presence of (*R*)-**1c** afforded *syn*-**4a** as the major product (Table 2, entry 4). In addition, both reactions proceeded with high chirality transfer in a retentive manner.

■ Chemical Models and Computational Methods for the Investigation of the Reaction Mechanism: DFT Study

In the reaction pathway for the present Petasis-Ferrier-type rearrangement as shown in Scheme 1, protonation of the oxygen atom of the vinyl ether moiety by catalyst (*R*)-**1** initiates C-O bond cleavage, affording the oxocarbenium intermediate **A** (R = Ph). Subsequent C-C bond formation furnishes the rearranged products *anti*- and *syn*-**3a**. Thus, *anti*- and *syn*-reaction pathways are accessible after the C-O bond cleavage step. Calculations were carried out for complexes of (*R*)-**2a** with (*R*)-**1a** and those of (*S*)-**2a** with (*R*)-**1c**. Each transition structure for the C-O bond cleavage and C-C bond formation steps were located individually. All of the atoms in the catalysts and the substrates were considered in the calculations without any simplification of the structures.

All calculations were performed with the Gaussian 09 package (Revision C.01).[22] The geometries were fully optimized and characterized using frequency calculations at the BHandHLYP/6-31G* level.[23] The solution-phase energies were evaluated using single-point energy calculations at the B3LYP-D/6-311+G** level[24] according to the polarized continuum model (CPCM, toluene, ε = 2.379)[25] for the optimized structures.

■ Analysis of the *Anti*-selective Reaction of (*R*)-**2a** Catalyzed by (*R*)-**1a**

First, the mechanism of the *anti*-selective reaction of (*R*)-**2a** catalyzed by (*R*)-**1a** was investigated. The energy profile of the reaction is shown in Fig. 2. The highest energy barrier in the energy profile is that of the C-O bond cleavage step (**TSr$_{co}$**), indicating that this step is the rate-determining step. The subsequent rotation of enol moiety primarily around the C5-C6 bond (see Fig. 3) through **TSr-int** led to intermediate **INTr2**, which is the precursor of the C-C bond formation.[26] Focusing on the stereodetermining C-C bond forming step, **TSr$_{cc}$-*anti***, which affords *anti*-**3a**, is more stable than **TSr$_{cc}$-*syn***, which affords *syn*-**3a**, by 1.4 kcal mol^{-1}.[27] Therefore, the *anti*-selective pathway is the more energetically favored pathway in Petasis-Ferrier-type rearrangement of (*R*)-**2a** catalyzed by (*R*)-**1a**, which is in agreement with the experimental results.

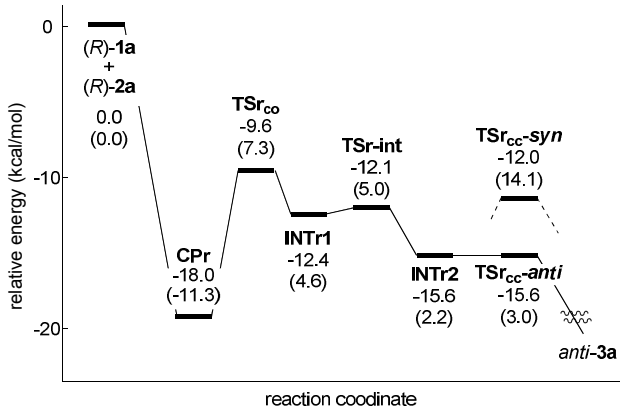

Fig. 2 Energy profile for the reaction of (*R*)-**2a** catalyzed by (*R*)-**1a**. The potential energy of the sum of (*R*)-**1a** and (*R*)-**2a** was set to zero. The energies for single-point calculations in the solution phase are shown. The energies for frequency calculations with the BHandHLYP/6-31G* level are indicated in parentheses.

Fig. 3 shows the 3D structures and schematic representation models of C-O bond cleavage and C-C bond forming steps. In each of the three transition structures, two P-O bonds of the phosphoric acid moiety are nearly the same length (1.48 - 1.50 Å). This results suggests that, rather than the phosphoric acid moiety consisting of a P-OH single bond and a P=O double bond, the phosphoric acid releases a proton as an anionic conjugate base, and the resultant negative charge is delocalized over the phosphoric acid moiety.[3] Therefore, the transition states can be regarded as a complex between the negatively charged conjugate base of the catalyst and the positively charged (protonated) substrate, which is stabilized by O-H···O hydrogen-bonding interactions between the enol moiety of the substrate and the phosphate moiety of the catalyst.

Detailed analysis of the transition structures revealed that the distances between the phosphoryl oxygen of the catalyst and the neighboring hydrogen atoms of the substrate are considerably shorter than the sum of the van der Waals radii of H and O atoms (ca. 2.7 Å), indicating the involvement of a non-classical C-H···O hydrogen bonding interaction.[12,28-31] Furthermore, two distinct types of C-H···O hydrogen bonds were identified in the transition structures. One is the hydrogen bond between the C-H bond of the oxocarbenium moiety and the oxygen atom of the catalyst (C-$H_{C=O}$···O in **TSr$_{co}$** and **TSr$_{cc}$-*anti***). The other is the bond between the C-H bond in the *ortho*-position of the phenyl ring and the oxygen atom of the catalyst (C-H_{Ph}···O in **TSr$_{co}$**, **TSr$_{cc}$-*anti***, and **TSr$_{cc}$-*syn***). The substrate is uniquely directed at the catalyst by the cooperative effect of the O-H···O and non-classical C-H···O hydrogen bonds.

To explain the origin of the *anti*-selectivity, the structures of **TSr$_{cc}$-*anti*** and **TSr$_{cc}$-*syn*** were compared. As indicated in Fig. 2, the energetically favored **TSr$_{cc}$-*anti***, which affords *anti*-**3a**, is stabilized by one O-H···O and two C-H···O hydrogen bonds (i.e., C-$H_{C=O}$···O and C-H_{Ph}···O). In contrast, the energetically disfavored **TSr$_{cc}$-*syn***, which affords *syn*-**3a**, is stabilized by only one O-H···O and one C-H_{Ph}···O bond, and lacks the C-$H_{C=O}$···O hydrogen bond. In **TSr$_{cc}$-*syn***, the C-H bond of the oxocarbenium moiety is oriented away from the catalyst and unable to form the C-H···O hydrogen bond. Presumably, other possible reaction pathways affording *syn*-**3a** are prevented due to the bulky substituents at the 3,3'-position of the catalyst.

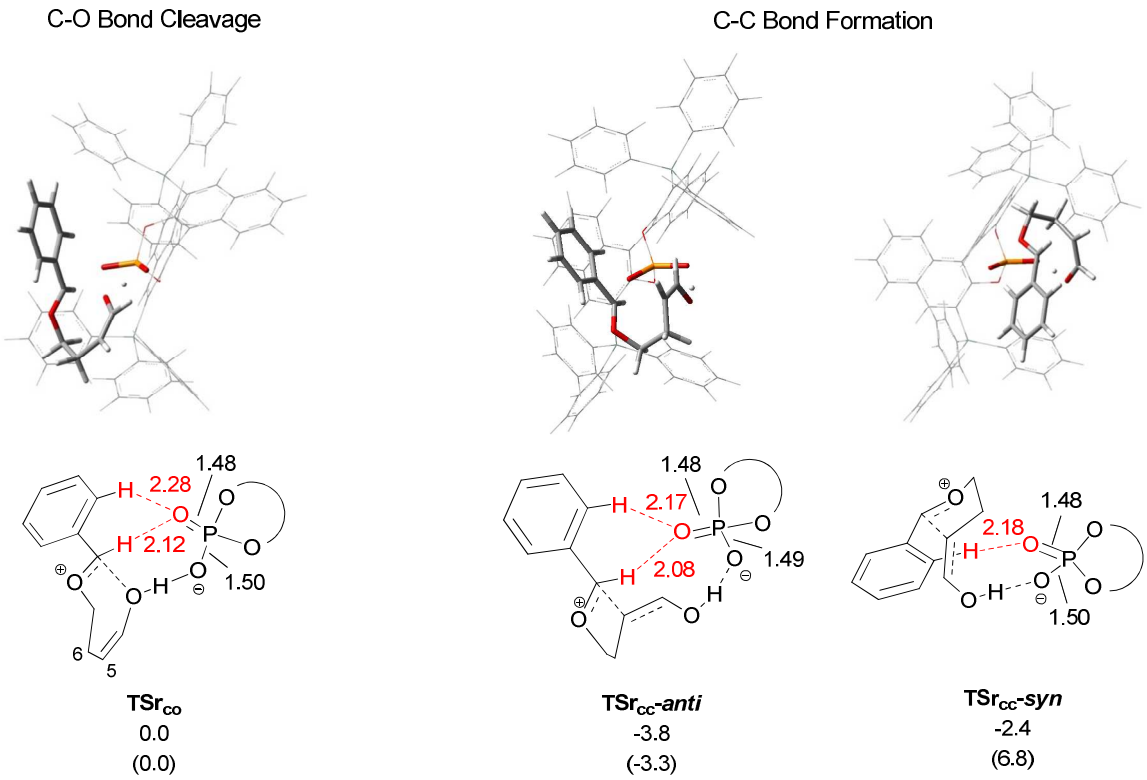

Fig. 3 3D structures and schematic representation models of **TSr$_{co}$**, **TSr$_{cc}$-*anti***, and **TSr$_{cc}$-*syn***. Bond lengths are indicated in Å. C-H···O hydrogen bonds are highlighted in red. The energies for single-point calculations in the solution phase are shown. The energies for frequency calculations with the BHandHLYP/6-31G* level are indicated in parentheses.

■ Analysis of *the Syn*-selective Reaction of (*S*)-**2a** Catalyzed by (*R*)-**1c**

Next, the mechanism of the *syn*-selective reaction of (*S*)-**2a** catalyzed by (*R*)-**1c** was investigated. The energy profile of the present reaction was similar to that illustrated in Fig. 2.[32] As is the case for the *anti*-selective reaction of (*R*)-**2a**, the highest energy barrier in the energy profile was that of the C-O bond cleavage step, indicating that this step is the rate-determining step. Focusing on the stereodetermining C-C bond forming step, it was found that **TSs$_{cc}$-*syn*** is more stable than **TSs$_{cc}$-*anti*** by 1.6 kcal mol^{-1}. Therefore, the *syn*-selective pathway is the more energetically favored pathway in the Petasis-Ferrier-type rearrangement of (*S*)-**2a** catalyzed by (*R*)-**1c**, which is in agreement with the experimental results.

Fig. 4 shows the 3D structures and schematic representation models of C-O bond cleavage and C-C bond forming steps. As shown in Fig. 4, the substrate structures for **TSs$_{cc}$-*anti*** and **TSs$_{cc}$-*syn*** are the mirror images of those for **TSr$_{cc}$-*anti*** and **TSr$_{cc}$-*syn***, respectively.[33] On the other hand, the structure for **TSs$_{co}$** is in sharp contrast to that of **TSr$_{co}$**. In **TSs$_{co}$**, the vinyl moiety, rather than the formyl moiety, of the substrate forms a C-H···O hydrogen bond with the phosphoryl oxygen of the catalyst. In addition, the C-H bond of *ortho*-position of the phenyl ring forms a C-H···O hydrogen bond with an ethereal oxygen of the phosphoric acid moiety.

To explain the origin of *syn*-selectivity, the structures of **TSs$_{cc}$-*syn*** and **TSs$_{cc}$-*anti*** were compared. The energetically disfavored **TSs$_{cc}$-*anti*** features one O-H···O and two C-H···O hydrogen bonds (i.e., C-H$_{C=O}$···O and C-H$_{Ph}$···O hydrogen bonds). However, the phenyl ring of the substrate and the 9-anthryl group of the catalyst are located close to one another, leading to steric congestion that may destabilize the transition state. On the other hand, **TSs$_{cc}$-*syn***, which is stabilized by only one O-H···O and one C-H···O hydrogen bond, is energetically favored compared to **TSs$_{cc}$-*anti***, despite the fact that the number of non-classical hydrogen bonding interactions is reduced. In **TSs$_{cc}$-*syn***, however, further stabilization can be expected due to π-π stacking interactions enabled by the parallel orientation of the phenyl group of the substrate and the 9-anthryl group of the catalyst at a distance of 3.5 Å.[34,35]

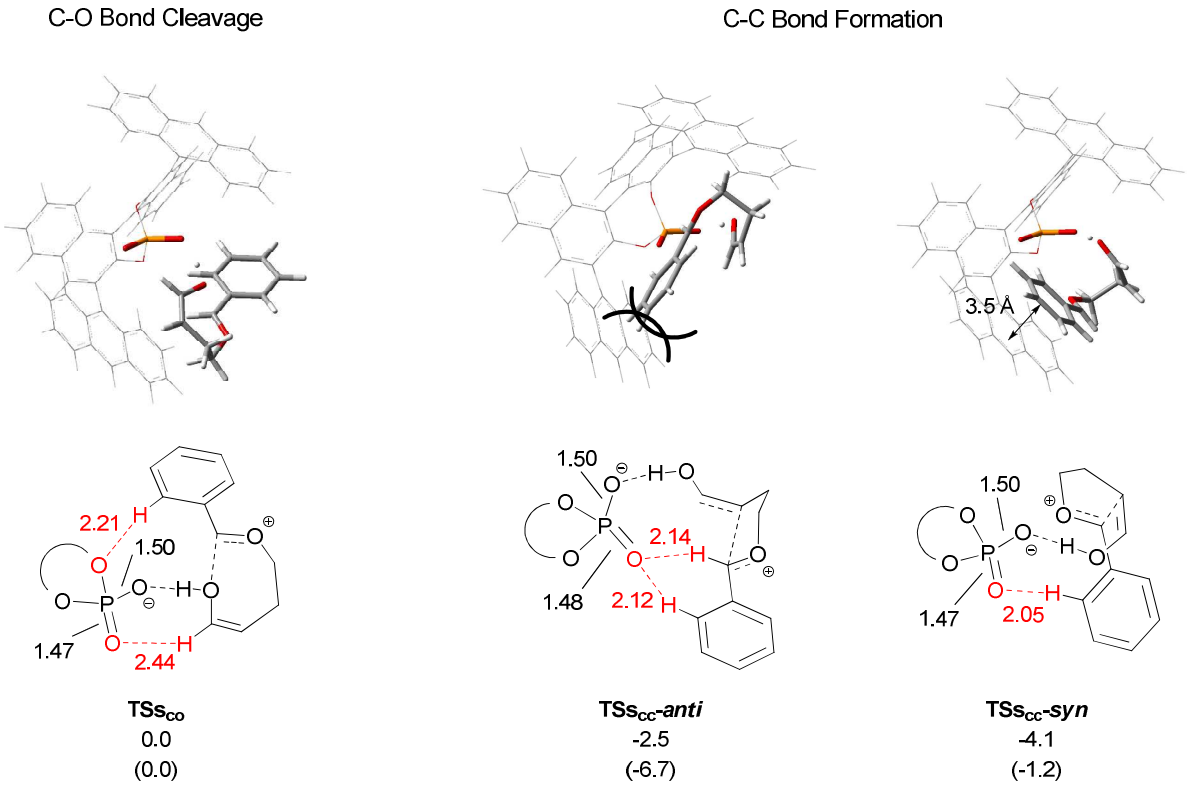

Fig. 4 3D structures and schematic representation models of **TSs$_{co}$**, **TSs$_{cc}$-*anti***, and **TSs$_{cc}$-*syn***. Bond lengths are indicated in Å. C-H···O hydrogen bonds are highlighted in red. The energies for single-point calculations in the solution phase are shown. The energies for frequency calculations with the BHandHLYP/6-31G* level are indicated in parentheses.

To confirm the stabilizing effect of this π-π stacking interaction in **TSs$_{cc}$-*syn***, a further analysis to evaluate the energy of interaction between the catalyst and the substrate was carried out.[36] Thus, a complex is divided into two fragments in order to evaluate the energy of interaction (E_{int}) between them. **TSs$_{cc}$-*syn*** was divided into the protonated substrate and deprotonated catalyst, and E_{int} between them was calculated using the following equation:

$$E_{int} = E(\textbf{TSs}_{cc}\textbf{-}\textit{syn}) - \{E(\text{substrate} + H^+) + E(\text{catalyst} - H^+)\}$$

where E(**TSs$_{cc}$-*syn***) is the total energy of **TSs$_{cc}$-*syn***, E(substrate + H$^+$) is the energy of the protonated substrate, and E(catalyst – H$^+$) is the energy of the deprotonated catalyst. E_{int} was also calculated for **F1** and **F2**, which were generated by replacing one of the 9-anthryl groups (Ar^1, Ar^2) of **TSs$_{cc}$-*syn*** with a hydrogen atom, respectively.[37] E_{int} of **F1** and **F2** were compared to that of **TSs$_{cc}$-*syn*** (Table 3, shown in parentheses). The absolute value of E_{int} decreased by 8.3 kcal mol^{-1} in **F1** and by 2.0 kcal mol^{-1} in **F2** compared to that of **TSs$_{cc}$-*syn*** for calculations at the B3LYP-D level (Table 3, entries 2 and 3). The dramatic change in E_{int} for **F1** can be attributed to the absence of the 9-anthryl group, which is thought to participate in a π-π stacking interaction with the substrate, as described above.

Table 3 Evaluation of the energy of interaction in **TSs$_{cc}$-*syn***

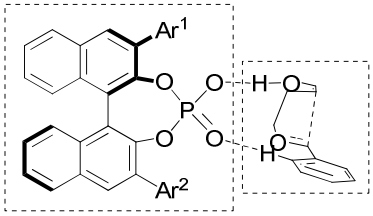

Entry		Ar^1	Ar^2	E_{int} (kcal mol^{-1})[a]	
				B3LYP-D[b]	BHandHLYP[c]
1	**TSs$_{cc}$-*syn***	9-anthryl	9-anthryl	-69.5 (0.0)	-110.7 (0.0)
2	**F1**	9-anthryl	H	-61.2 (+8.3)	-107.8 (+2.9)
3	**F2**	H	9-anthryl	-67.5 (+2.0)	-110.9 (-0.2)

[a] The relative values of E_{int} with respect to that of **TSs$_{cc}$-*syn*** are indicated in parentheses. [b] CPCM(toluene)/B3LYP-D/6-311+G**. [c] BHandHLYP/6-31G*.

Notably, the change of E_{int} for **F1** calculated at the BHandHLYP level is much smaller than that calculated at the B3LYP-D level (Table 3, entry 2). In general, the BHandHLYP method does not correctly evaluate the dispersion interactions, which is the origin of π-π stacking structure.[38] It should also be noted that the transition energies calculated at

the BHandHLYP level did not predict the experimental results correctly (Fig. 3, in parentheses. **TSs$_{cc}$-*syn*** is 5.5 kcal mol^{-1} less stable than **TSs$_{cc}$-*anti*** for the BHandHLYP calculation).[39] The inaccurate evaluation of the transition energy at the BHandHLYP level, combined with the results shown in Table 3, strongly suggest the involvement of the dispersion interaction as a stabilizing factor in the present catalytic reaction.[34,35,38,39] The *syn*-selectivity observed when using (*R*)-**1c** with (*S*)-**2a** can be rationalized as the result of a π-π stacking interaction between the substrate and the anthryl group of the catalyst.

CONCLUSION

The Petasis-Ferrier-type rearrangement of cyclic vinyl acetal **2a** catalyzed by (*R*)-**1** was investigated as a model reaction for clarifying the stereocontrolling element in reactions catalyzed by chiral phosphoric acid catalysts that proceed without the formation of X-H···A-type hydrogen bonds to electrophilic species. The reaction of (*R*)-**2a** catalyzed by (*R*)-**1a** selectively afforded *anti*-**4a**, while the reaction of (*S*)-**2a** catalyzed by (*R*)-**1c** selectively afforded *syn*-**4a**. Both reactions proceeded with high chirality transfer in a retentive manner. DFT studies of the present catalytic reaction revealed that non-classical C-H···O hydrogen bonds are crucial in achieving high stereocontrol. In other words, C-H···O hydrogen bonds play an alternative to X-H···A-type hydrogen bonds as a stereocontrolling element in ion-pairing interactions.[31] It was also revealed that the 9-anthryl group at the 3,3'-position of the catalyst stabilized the transition state through π-π stacking interactions. Such an attractive interaction between a catalyst substituent and the substrate is in sharp contrast to well-understood repulsive interactions induced by steric bulkiness. Development of novel catalytic asymmetric reactions that harnesse these newly revealed stereocontrolling elements is now under way in our laboratory.

Acknowledgements

This work was partially supported by a Grant-in-Aid for Scientific Research on Innovative Areas 'Advanced Molecular Transformations by Organocatalysts' from MEXT, Japan (Grant No. 23105002). We also thank the JSPS for a Research Fellowship for Young Scientists (K.K. and Y.T.).

Notes and References

[a] Department of Chemistry, Graduate School of Science, Tohoku University, Aoba-ku, Sendai 980-8578, Japan
E-mail: mterada@m.tohoku.ac.jp
Fax: +81-22-795-6602; Tel: +81-22-795-6602
[b] Department of Chemistry and Research Center for Smart Molecules, Faculty of Science, Rikkyo University, Nishi-Ikebukuro, Toshima-ku, Tokyo 171-8501, Japan
[c] National Institute of Advanced Industrial Science and Technology (AIST), Tsukuba, Ibaraki 305-8568, Japan
[d] Research and Analytical Center for Giant Molecules, Graduate School of Science, Tohoku University, Aoba-ku, Sendai 980-8578, Japan

† Electronic supplementary information (ESI) available: Representative experimental procedure, spectroscopic data, X-ray crystallographic data, computational details (Cartesian coordinates and absolute energies for stationary points). See DOI: 10.1039/b000000x/

1 For selected reviews of chiral Brønsted acid catalysis, see: (a) P. M. Pihko, *Angew. Chem. Int. Ed.*, 2004, **43**, 2062; (b) T. Akiyama, J. Itoh and K. Fuchibe, *Adv. Synth. Catal.*, 2006, **348**, 999; (c) T. Akiyama, *Chem. Rev.*, 2007, **107**, 5744; (d) M. S. Taylor and E. N. Jacobsen, *Angew. Chem. Int. Ed.*, 2006, **45**, 1520; (e) A. G. Doyle and E. N. Jacobsen, *Chem. Rev.*, 2007, **107**, 5713; (f) D. Kampen, C. M. Reisinger and B. List, *Top. Curr. Chem.*, 2010, **291**, 395; (g) H. Yamamoto and N. Payette in *Hydrogen Bonding in Organic Synthesis* ed. P. M. Pihko, Wiley-VCH, Weinheim, 2009, p. 73; (h) C. H. Cheon and H. Yamamoto, *Chem. Commun.*, 2011, **47**, 3043; (i) S. Schenker, A. Zamfir, M. Freund and S. B. Tsogoeva, *Eur. J. Org. Chem.*, 2011, 2209.

2 For selected reviews of chiral phosphoric acid catalysis, see: (a) M. Terada, *Chem. Commun.*, 2008, 4097; (b) M. Terada, *Bull. Chem. Soc. Jpn.*, 2010, **83**, 101; (c) M. Terada, *Synthesis*, 2010, 1929; (d) M. Terada, *Curr. Org. Chem.*, 2011, **15**, 2227; (e) A. Zamfir, S. Schenker, M. Freund and S. B. Tsogoeva, *Org. Biomol. Chem.*, 2010, **8**, 5262; (f) T. Akiyama, in *Science of Synthesis, Asymmetric Organocatalysis 2, Brønsted Base and Acid Catalysts, and Additional Topics*, ed. K. Maruoka, Georg Thieme Verlag KG, New York, 2012, p. 169; (g) M. Terada and N. Momiyama, in *Science of Synthesis, Asymmetric Organocatalysis 2, Brønsted Base and Acid Catalysts, and Additional Topics*, ed. K. Maruoka, Georg Thieme Verlag KG, New York, 2012, p. 219. For seminal studies, see: (h) T. Akiyama, J. Itoh, K. Yokota and K. Fuchibe, *Angew. Chem. Int. Ed.*, 2004, **43**, 1566; (i) D. Uraguchi and M. Terada, *J. Am. Chem. Soc.*, 2004, **126**, 5356.

3 (a) M. Yamanaka, J. Itoh, K. Fuchibe and T. Akiyama, *J. Am. Chem. Soc.*, 2007, **129**, 6756; (b) M. Yamanaka and T. Hirata, *J. Org. Chem.*, 2009, **74**, 3266; (c) T. Akiyama, H. Morita, P. Bachu, K. Mori, M. Yamanaka and T. Hirata, *Tetrahedron*, 2009, **65**, 4950; (d) K. Mori, T. Katoh, T. Suzuki, T. Noji, M. Yamanaka and T. Akiyama, *Angew. Chem. Int. Ed.*, 2009, **48**, 9652; (e) T. Hirata and M. Yamanaka, *Chem.-Asian J.*, 2011, **6**, 510; (f) M. Yamanaka, M. Hoshino, T. Katoh, K. Mori and T. Akiyama, *Eur. J. Org. Chem.*, 2012, 4508; (g) K. Mori, Y. Ichikawa, M. Kobayashi, Y. Shibata, M. Yamanaka and T. Akiyama, *Chem. Sci.*, 2013, **4**, 4235; (h) K. Saito, Y. Shibata, M. Yamanaka and T. Akiyama, *J. Am. Chem. Soc.*, 2013, **135**, 11740; (i) K. Mori, Y. Ichikawa, M. Kobayashi, Y. Shibata, M. Yamanaka and T. Akiyama, *J. Am. Chem. Soc.*, 2013, **135**, 3964; (j) Y. Shibata and M. Yamanaka, *J. Org. Chem.*, 2013, **78**, 3731.

4 (a) L. Simón and J. M. Goodman, *J. Am. Chem. Soc.*, 2008, **130**, 8741; (b) L. Simón and J. M. Goodman, *J. Am. Chem. Soc.*, 2009, **131**, 4070; (c) L. Simón and J. M. Goodman, *J. Org. Chem.*, 2010, **75**, 589; (d) L. Simón and J. M. Goodman, *J. Org. Chem.*, 2011, **76**, 1775.

5 (a) X.-H. Chen, Q. Wei, S.-W. Luo, H. Xiao and L.-Z. Gong, *J. Am. Chem. Soc.*, 2009, **131**, 13819; (b) N. Li, X.-H. Chen, J. Song, S.-W. Luo, W. Fan and L.-Z. Gong, *J. Am. Chem. Soc.*, 2009, **131**, 15301;

(c) L. He, X.-H. Chen, D.-N. Wang, S.-W. Luo, W.-Q. Zhang, J. Yu, L. Ren and L.-Z. Gong, *J. Am. Chem. Soc.*, 2011, **133**, 13504; (d) F. Shi, S.-W. Luo, Z.-L. Tao, L. He, J. Yu, S.-J. Tu and L.-Z. Gong, *Org. Lett.*, 2011, **13**, 4680; (e) F. Shi, G.-J. Xing, Z.-L. Tao, S.-W. Luo, S.-J. Tu and L.-Z. Gong, *J. Org. Chem.*, 2012, **77**, 6970.

6 (a) T. Marcelli, P. Hammar and F. Himo, *Chem.-Eur. J.*, 2008, **14**, 8562; (b) T. Marcelli, P. Hammar and F. Himo, *Adv. Synth. Cat.*, 2009, **351**, 525.

7 F.-Q. Shi and B.-A. Song, *Org. Biomol. Chem.*, 2009, **7**, 1292.

8 (a) Q.-A. Cai, C. Zheng and S.-L. You, *Angew. Chem. Int. Ed.*, 2010, **49**, 8666; (b) C. Zheng, Y.-F. Sheng, Y.-X. Li and S.-L. You, *Tetrahedron*, 2010, **66**, 2875.

9 S. Xu, Z. Wang, Y. Li, X. Zhang, H. Wang and K. Ding, *Chem.-Eur. J.*, 2010, **16**, 3021.

10 For selected examples of the generation of cationic electrophiles by chiral phosphoric acid catalysts and their analogues, see: (a) N. J. A. Martin and B. List, *J. Am. Chem. Soc.*, 2006, **128**, 13368; (b) S. Mayer and B. List, *Angew. Chem. Int. Ed.*, 2006, **45**, 4193; (c) X. Wang and B. List, *Angew. Chem. Int. Ed.*, 2008, **47**, 1119; (d) M. J. Wanner, R. N. S. van der Haas, K. R. de Cuba, J. H. van Maarseveen and H. Hiemstra, *Angew. Chem. Int. Ed.*, 2007, **46**, 7485; (e) G. L. Hamilton, T. Kanai and F. D. Toste, *J. Am. Chem. Soc.*, 2008, **130**, 14984; (f) M. Rueping, B. J. Nachtsheim, S. A. Moreth and M. Bolte, *Angew. Chem. Int. Ed.*, 2008, **47**, 593; (g) M. Rueping, U. Uria, M.-Y. Lin and I. Atodiresei, *J. Am. Chem. Soc.*, 2011, **133**, 3732; (h) M. E. Muratore, C. A. Holloway, A. W. Pilling, R. I. Storer, G. Trevitt and D. J. Dixon, *J. Am. Chem. Soc.*, 2009, **131**, 10796; (i) C. A. Holloway, M. E. Muratore, R. I. Storer and D. J. Dixon, *Org. Lett.*, 2010, **12**, 4720; (j) Q.-W. Zhang, C.-A. Fan, H.-J. Zhang, Y.-Q. Tu, Y.-M. Zhao, P. Gu and Z.-M. Chen, *Angew. Chem. Int. Ed.*, 2009, **48**, 8572; (k) G. Bergonzini, S. Vera and P. Melchiorre, *Angew. Chem. Int. Ed.*, 2010, **49**, 9685; (l) T. Liang, Z. J. Zhang and J. C. Antilla, *Angew. Chem. Int. Ed.*, 2010, **49**, 9734; (m) Z.-Y. Han, R. Guo, P.-S. Wang, D.-F. Chen, H. Xiao and L.-Z. Gong, *Tetrahedron Lett.*, 2011, **52**, 5963; (n) E. Aranzamendi, N. Sotomayor and E. Lete, *J. Org. Chem.*, 2012, **77**, 2986; (o) B. Y. Guo, G. Schwarzwalder and J. T. Njardarson, *Angew. Chem. Int. Ed.*, 2012, **51**, 5675; (p) Z. K. Sun, G. A. Winschel, A. Borovika and P. Nagorny, *J. Am. Chem. Soc.*, 2012, **134**, 8074; (q) M. Terada, T. Yamanaka and Y. Toda, *Chem.-Eur. J.*, 2013, **19**, 13658.

11 These reactions are often termed chiral anion catalysis (Ref. 11e), asymmetric counteranion-directed catalysis (Ref. 11g), or ion-pairing catalysis (ref. 11h). For reviews, see: (a) J. Lacour and V. Hebbe-Viton, *Chem. Soc. Rev.*, 2003, **32**, 373; (b) J. Lacour and D. Moraleda, *Chem. Commun.*, 2009, 7073; (c) E. P. Ávila and G. W. Amarante, *Chemcatchem*, 2012, **4**, 1713; (d) A. Parra, S. Reboredo, A. M. M. Castro and J. Alemán, *Org. Biomol. Chem.*, 2012, **10**, 5001; (e) R. J. Phipps, G. L. Hamilton and F. D. Toste, *Nat. Chem.*, 2012, **4**, 603; (f) M. Mahlau and B. List, *Isr. J. Chem.*, 2012, **52**, 630; (g) M. Mahlau and B. List, *Angew. Chem. Int. Ed.*, 2013, **52**, 518; (h) K. Brak and E. N. Jacobsen, *Angew. Chem. Int. Ed.*, 2013, **52**, 534.

12 The crucial role of C-H···O hydrogen bonds as stereocontrolling elements in ion-pairs was proposed for phase-transfer catalysis. See: (a) T. Ohshima, T. Shibuguchi, Y. Fukuta and M. Shibasaki, *Tetrahedron*, 2004, **60**, 7743; (b) E. Gomez-Bengoa, A. Linden, R. López, I. Múgica-Mendiola, M. Oiarbide and C. Palomo, *J. Am. Chem. Soc.*, 2008, **130**, 7955; (c) E. Yamamoto, D. Gokuden, A. Nagai, T. Kamachi, K. Yoshizawa, A. Hamasaki, T. Ishida and M. Tokunaga, *Org. Lett.*, 2012, **14**, 6178; (d) T. Kamachi and K. Yoshizawa, *Org. Lett.*, 2014, **16**, 472. The importance of C-H···O hydrogen bonds in ion-pairs was also suggested in the reactions using DMAP-type nucleophilic catalysts. See: (e) E. Larionov, F. Achrainer, J. Humin and H. Zipse, *ChemCatChem*, 2012, **4**, 559; (f) R. Nishino, T. Furuta, K. Kan, M. Sato, M. Yamanaka, T. Sasamori, N. Tokitoh and T. Kawabata, *Angew. Chem., Int. Ed.*, 2013, **52**, 6445.

13 Although interaction between neutral electrophiles and chiral phosphoric acid catalysts has been well studied by DFT calculation (Fig. 1a, ref. 3-9), no computational analysis has been reported to date on the interaction between cationic electrophiles that lack Brønsted basic sites and the anionic conjugate base of chiral phosphoric acid catalysts (Fig. 1b).

14 For seminal studies of Petasis-Ferrier rearrangement, see: (a) N. A. Petasis and S.-P. Lu, *J. Am. Chem. Soc.*, 1995, **117**, 6394; (b) N. A. Petasis and S.-P. Lu, *Tetrahedron Lett.*, 1996, **37**, 141.

15 For a computational study of the mechanism of Petasis-Ferrier rearrangement, see: G.-J. Jiang, Y. Wang and Z.-X. Yu, *J. Org. Chem.*, 2013, **78**, 6947.

16 For Lewis acid-catalyzed Petasis-Ferrier-type rearrangement of 7-membered cyclic vinyl acetals, see: (a) H. Suzuki, H. Yashima, T. Hirose, M. Takahashi, Y. Morooka and T. Ikawa, *Tetrahedron Lett.*, 1980, **21**, 4927; (b) K. Samizu and K. Ogasawara, *Chem. Lett.*, 1995, 543; (c) H. Frauenrath and T. Philipps, *Tetrahedron*, 1986, **42**, 1135; (d) H. Frauenrath and J. Runsink, *J. Org. Chem.*, 1987, **52**, 2707; (e) S. Takano, K. Samizu and K. Ogasawara, *Synlett*, 1993, 785; (f) C. G. Nasveschuk, N. T. Jui and T. Rovis, *Chem. Commun.*, 2006, 3119; (g) C. G. Nasveschuk and T. Rovis, *J. Org. Chem.*, 2008, **73**, 612; (h) C. G. Nasveschuk and T. Rovis, *Synlett*, 2008, 126. For a Brønsted acid-catalyzed reaction, see: (i) O. Kubo, K. Yahata, T. Maegawa and H. Fujioka, *Chem. Commun.*, 2011, **47**, 9197.

17 (a) A. B. Smith, III, P. R. Verhoest, K. P. Minbiole and J. J. Lim, *Org. Lett.*, 1999, **1**, 909; (b) A. B. Smith, III, K. P. Minbiole, P. R. Verhoest and T. J. Beauchamp, *Org. Lett.*, 1999, **1**, 913; (c) Y. D. Zhang, N. T. Reynolds, K. Manju and T. Rovis, *J. Am. Chem. Soc.*, 2002, **124**, 9720.

18 See ESI† for determination of the absolute configurations.

19 *Anti*-**3a** was confirmed to be a kinetically formed product for Table 1, entry 4 and Table 2, entry 1. See ESI† for details.

20 The reaction of (*R*)-**2a** using 5 mol% of diphenyl phosphate as the catalyst was also conducted in toluene for 10 min to afford the product in 90% yield with *anti*:*syn* = 37 (66% ee) : 63 (83% ee).

21 When the reaction was run for 1 h, the diastereoselectivity decreased to *anti*:*syn* = 11:89, while the enantiomeric purity of *syn*-**4a** was conserved. This result indicates that the rearranged product *syn*-**3a** gradually epimerizes to *anti*-**3a** under the present reaction conditions.

22 Gaussian 09, Revision C.01; M. J. Frisch, G. W. Trucks, H. B. Schlegel, G. E. Scuseria, M. A. Robb, J. R. Cheeseman, G. Scalmani, V. Barone, B. Mennucci, G. A. Petersson, H. Nakatsuji, M. Caricato, X. Li, H. P. Hratchian, A. F. Izmaylov, J. Bloino, G. Zheng, J. L. Sonnenberg, M. Hada, M. Ehara, K. Toyota, R. Fukuda, J. Hasegawa, M. Ishida, T. Nakajima, Y. Honda, O. Kitao, H. Nakai, T. Vreven, J. A. Montgomery, Jr., J. E. Peralta, F. Ogliaro, M. Bearpark, J. J. Heyd, E. Brothers, K. N. Kudin, V. N. Staroverov, T. Keith, R. Kobayashi, J.

Normand, K. Raghavachari, A. Rendell, J. C. Burant, S. S. Iyengar, J. Tomasi, M. Cossi, N. Rega, J. M. Millam, M. Klene, J. E. Knox, J. B. Cross, V. Bakken, C. Adamo, J. Jaramillo, R. Gomperts, R. E. Stratmann, O. Yazyev, A. J. Austin, R. Cammi, C. Pomelli, J. W. Ochterski, R. L. Martin, K. Morokuma, V. G. Zakrzewski, G. A. Voth, P. Salvador, J. J. Dannenberg, S. Dapprich, A. D. Daniels, O. Farkas, J. B. Foresman, J. V. Ortiz, J. Cioslowski, and D. J. Fox, Gaussian, Inc., Wallingford CT, 2010.

23 A. D. Becke, *J. Chem. Phys.*, 1993, **98**, 1372.

24 (a) C. Lee, W. T. Yang and R. G. Parr, *Phys. Rev. B: Condens. Matter Mater. Phys.*, 1988, **37**, 785; (b) A. D. Becke, *J. Chem. Phys.*, 1993, **98**, 5648; (c) S. Grimme, *J. Comput. Chem.*, 2006, **27**, 1787.

25 V. Barone and M. Cossi, *J. Phys. Chem. A*, 1998, **102**, 1995.

26 See ESI† for the structure of **CPr** (hydrogen-bonding complex), **TSr-int** (transition state of bond rotation), **INTr1** and **INTr2** (stable intermediates).

27 Although **INTr2** (stable intermediate) was slightly stable than **TSr$_{cc}$-*anti*** in BHandHLYP/6-31G* (0.8 kcal/mol), the energies of these two states in single-point calculation were almost the same. **INTr2** can be considered as a transition state with very low energy barrier or an inflection point in CPCM(toluene)/B3LYP-D/6-311+G**.

28 For reviews of C-H···O hydrogen bond as a stereocontrolling element, see: (a) E. J. Corey and T. W. Lee, *Chem. Commun.*, 2001, 1321; (b) R. K. Castellano, *Curr. Org. Chem.*, 2004, **8**, 845; (c) R. C. Johnston and P. H.-Y. Cheong, *Org. Biomol. Chem.*, 2013, **11**, 5057.

29 Computational studies suggested the involvement of C-H···O hydrogen bond as stereocontrolling elements in certain chiral phosphoric acid-catalyzed reactions. For allylboration and propargylation of aldehydes, see: (a) M. N. Grayson, S. C. Pellegrinet and J. M. Goodman, *J. Am. Chem. Soc.*, 2012, **134**, 2716; (b) M. N. Grayson and J. M. Goodman, *J. Am. Chem. Soc.*, 2013, **135**, 6142; (c) H. Wang, P. Jain, J. C. Antilla and K. N. Houk, *J. Org. Chem.*, 2013, **78**, 1208. For aza-Claisen rearrangement, see: (d) P. Maity, R. P. Pemberton, D. J. Tantillo and U. K. Tambar, *J. Am. Chem. Soc.*, 2013, **135**, 16380.

30 The interaction *via* C-H···O hydrogen bonds was also proposed in the following chiral phosphoric acid-catalyzed reactions; (a) M. Terada, K. Soga and N. Momiyama, *Angew. Chem. Int. Ed.*, 2008, **47**, 4122; (b) M. Terada, H. Tanaka and K. Sorimachi, *J. Am. Chem. Soc.*, 2009, **131**, 3430; (c) N. Momiyama, H. Tabuse and M. Terada, *J. Am. Chem. Soc.*, 2009, **131**, 12882; (d) I. Čorić, S. Vellalath and B. List, *J. Am. Chem. Soc.*, 2010, **132**, 8536; (e) L. R. Reddy, *Org. Lett.*, 2012, **14**, 1142. For C-H···N and C-H···F interactions in stable reaction intermediates in a chiral triflyl thiophosphoramide-catalyzed reaction, see; (f) C. Lu, X. Su and P. E. Floreancig, *J. Org. Chem.*, 2013, **78**, 9366.

31 Both X-H···A-type and C-H···O hydrogen bonds primarily originate from electrostatic interactions. In this regard, C-H···O hydrogen bonds are inherently similar to X-H···A-type hydrogen bonds. See: (a) G. R. Desiaju, *Acc. Chem. Res.*, 1996, **29**, 441; (b) A. D. Buckingham, in *Theoretical Treatments of Hydrogen Bonding*, ed. D. Hadži, John Wiley & Sons Ltd, Chichester, 1997, p. 1, and references sited therein.

32 See ESI† for the energy profile and the structures of stable intermediates.

33 See ESI† for the structural comparison between **TSr$_{cc}$-*anti*** and **TSs$_{cc}$-*anti***, **TSr$_{cc}$-*syn*** and **TSs$_{cc}$-*syn***, respectivery.

34 Very recently, the involvement of π-π stacking interaction as a stereocontrolling element in a chiral phosphoric acid-catalyzed reaction was proposed. See: J. Calleja, A. B. González-Pérez, Á. R. de Lera, R. Álvarez, F. J. Fañanás and F. Rodríguez, *Chem. Sci.*, 2014, **5**, 996. Also see ref. 3a.

35 For reviews of aromatic interactions as stereocontrolling elements, see: (a) G. B. Jones and B. J. Chapman, *Synthesis*, 1995, 475; (b) E. A. Meyer, R. K. Castellano and F. Diederich, *Angew. Chem., Int. Ed.*, 2003, **42**, 1210; (c) L. M. Salonen, M. Ellermann and F. Diederich, *Angew. Chem. Int. Ed.*, 2011, **50**, 4808; (d) E. H. Krenske, *Org. Biomol. Chem.*, 2013, **11**, 5226; (e) E. H. Krenske and K. N. Houk, *Acc. Chem. Res.*, 2013, **46**, 979.

36 (a) E. Nakamura, M, Nakamura, Y. Miyachi, N. Koga and K. Morokuma, *J. Am. Chem. Soc.*, 1993, **115**, 99, and references sited therein; (b) W. Nakanishi, M. Yamanaka and E. Nakamura, *J. Am. Chem. Soc.*, 2005, **127**, 1446; (c) S. Nakamura, C.-L. Liu, A. Muranaka and M. Uchiyama, *Chem.-Eur. J.*, 2009, **15**, 5686. Also see Ref. 3a.

37 See ESI† for the structure of **F1** and **F2**.

38 For theoretical evaluation of dispersion interactions, see: (a) P. Hobza, H. L. Selzle and E. W. Schlab, *J. Phys. Chem.*, 1996, **100**, 18790; (b) G. B. McGaughey, M. Gagné and A. K. Rappé, *J. Biol. Chem.*, 1998, **273**, 15458; (c) K. S. Kim, P. Tarakeshwar and J. Y. Lee, *Chem. Rev.*, 2000, **100**, 4145; (d) S. Tsuzuki, K. Honda, T. Uchimaru, M. Mikami and K. Tanabe, *J. Am. Chem. Soc.*, 2002, **124**, 104; (e) C. Romero, L. Fomina and S. Fomine, *Int. J. Quant. Chem.*, 2005, **102**, 200; (f) M. P. Waller, A. Robertazzi, J. A. Platts, D. E. Hibbs and P. A. Williams, *J. Comput. Chem.*, 2006, **27**, 491; (g) Y. Wei, I. Held and H. Zipse, *Org. Biomol. Chem.*, 2006, **4**, 4223; (h) Y. Zhao and D. G. Truhlar, *J. Chem. Theory Comput.*, 2007, **3**, 289; (i) H. Kruse, L. Goerigk and S. Grimme, *J. Org. Chem.*, 2012, **77**, 10824; (j) *Acc. Chem. Res.*, 2013, **46**: Special issue of aromatic interactions.

39 An inaccurate prediction of transition energies using a traditional functional was also reported in the literature. See: A. M. R. Smith, H. S. Rzepa, A. J. P. White, D. Billen and K. K. Hii, *J. Org. Chem.*, 2010, **75**, 3085.